https://doi.org/10.15407/ufm.22.04.511

NGUYEN QUANG HOC [1,*], BUI DUC TINH [1,], NGUYEN DUC HIEN [2], and LE HONG VIET [3]**

[1] Hanoi National University of Education, 136 Xuan Thuy, Hanoi, Vietnam
[2] Mac Dinh Chi High School, Chu Pah District, Gia Lai Province, Vietnam
[3] Tran Quoc Tuan University, Co Dong, Son Tay Town, Hanoi, Vietnam

* hocnq@hnue.edu.vn, ** tinhbd@hnue.edu.vn

ON THE JUMPS OF VOLUME, ENTHALPY AND ENTROPY AT THE MELTING POINT, THE THERMAL CONDUCTIVITY AND THERMAL DIFFUSIVITY FOR F.C.C. Au: THE TEMPERATURE- AND PRESSURE-DEPENDENCES

The melting temperature, the jumps of volume, enthalpy and entropy at the melting point, the isothermal compressibility, the thermal expansion coefficient, the heat capacity at constant volume, the Grüneisen parameter, the Debye temperature, the electrical resistivity, the thermal conductivity, and the thermal diffusivity for defective and perfect f.c.c. metals are studied by combining the statistical moment method (SMM), the limiting condition of the absolute stability of the crystalline state, the Clapeyron–Clausius equation, the Debye model, the Grüneisen equation, the Wiedemann–Franz law and the Mott equation. Numerical calculations are carried out for Au under high temperature and pressure. Calculated melting curve of Au is in a good agreement with experiments and other calculations. Obtained results are predictive and orient towards new experiments.

Keywords: jumps of volume, enthalpy and entropy at the melting point, thermal conductivity, thermal diffusivity, statistical moment method.

1. Introduction

Gold is a metal with high ductility, and structural stability under extreme pressure and temperature conditions [1, 2]. Au has a face-centred cubic structure (f.c.c.), which is stable at pressure $P = 600$ GPa and

Citation: Nguyen Quang Hoc, Bui Duc Tinh, Nguyen Duc Hien, and Le Hong Viet, On the Jumps of Volume, Enthalpy and Entropy at the Melting Point, the Thermal Conductivity and Thermal Diffusivity for F.C.C. Au: the Temperature- and Pressure-Dependences, *Progress in Physics of Metals*, **22**, No. 4: 511–530 (2021)

ambient temperature [3]. Au is widely used in industries such as photocatalysis for drugs [4]. Currently, there are many methods to study Au materials including experimental methods [5, 6], theoretical methods [7–11], ab initio calculations [12–14], energy approach quantification [15], the Z method [16], the Lindemann method [17–19], the molecular dynamics (MD) simulation [20] and the embedded atomic method (EAM) [21]. Several thermodynamic models have been used to describe the melting temperature as the Pawlow model, the Rie model [22] and the model of Reiss and Wilson [23]. The studies on the melting of Au are not complete. Experiments of laser heated diamond anvil cell (LH DAC) [24] and shock wave (SW) [25] provide the high-pressure melting curve of Au. The various possible experimental methods have been compared and measurements of the melting points of small gold particles have been made using a scanning electron-diffraction technique. This method was applied to particles having diameters down to 20 E. Consideration of the size distribution over an entire sample makes it necessary to carry out a careful analysis of the experimental results in order to deduce the melting temperature of particles having a well-defined diameter. The experimental results are quantitatively in good agreement with two phenomenological models. The first model describes the equilibrium condition for a system formed by a solid particle, a liquid particle having the same mass, and their saturating vapour phase. The second model assumes the pre-existence of a liquid layer surrounding the solid particle and describes the equilibrium of such a system in the presence of the vapour phase [26]. The relationship between the melting temperature and the particle size using a micro-electromechanical system (MEMS) was determined in [27]. At pressure P = 0.1 MPa, Au has a face-centred cubic (f.c.c.) structure with lattice constant a = 4.0785 Å at room temperature and melting point at T_m = 1337 K. The melting temperature of Au is also determined by theoretical calculations [28-30]. The phase transition temperature curves were determined up to T = = 1673 K and P = 6.5 GPa with the slope dT/dP = 60 K/GPa [31, 32] and up to T = 1923 K at P = 12 GPa [33]. According to [8], shock-induced melting begins to occur at pressure P = 120 GPa. Based on experimental and theoretical results, the melting temperature always depends linearly on the size of the material [34, 35]. Finally, according to [36–38] it is not possible to determine the melting temperature of materials with sizes $d < 5$ nm. Besides, because the complexity of experimental methods, the melting temperatures have limited value and do not guarantee high accuracy [39, 40]. There are many theoretical models such as the ab initio method and MD simulation based on Lindemann's law to predict high-pressure melting temperatures of metals. However, such approaches do not guarantee the evaluation of melting at extremely high temperatures and pressures [41–43]. Thermodynamic models based

on equations of state can predict the properties of solids [44–46] such as f.c.c.–h.c.p. structure transition at P = 240 GPa, T = 1000 K [47]. Determining the melting curve by experimental methods still has many limitations. The measuring devices are limited to pressure P = 35 GPa and experimental results above P = 15 GPa are scattered [48, 49, 50]. In addition, the influence of material size, energy and atomic number on structural characteristics, electronic structure and phase transition of metals and alloys is studied in [51–61]. The melting temperature has great influence on physical quantities such as the volume, the enthalpy, the entropy, the electrical resistivity, the Debye temperature, the thermal conductivity and the thermal diffusivity of materials [62–67]. In this paper, analytical expressions of the Helmholtz free energy, the cohesive energy, the crystal parameters, the nearest neighbour distance, the equilibrium vacancy concentration drum, the limit temperature of absolute stability for crystalline state, the melting temperature, the jumps of volume, enthalpy and entropy, the isothermal compressibility, the thermal expansion coefficient, the heat capacity at constant volume, the Grüneisen parameter, the Debye temperature, the thermal conductivity and the thermal diffusivity for f.c.c. perfect and defect metals are derived by combining the statistical moment method, the absolute stability conditions of crystalline state, the Clapeyron–Clausius equation, the Debye model, the Grüneisen equation, the Wiedemann–Franz law and the Mott equation. Our numerical calculations of the obtained theoretical results are performed for Au.

2. Model and Results

2.1. Theoretical Calculations

The Helmholtz free energy of the f.c.c. metals is equal to [68]

$$\psi = U_0 + \psi_0 + 3N\left\{\frac{\theta^2}{k^2}\left[\gamma_2 Y^2 - \frac{2\gamma_1}{3}\left(1+\frac{Y}{2}\right)\right] + \right.$$

$$\left. + \frac{2\theta^3}{k^4}\left[\frac{4}{3}\gamma_2^2 Y\left(1+\frac{Y}{2}\right) - 2(\gamma_1^2 + 2\gamma_1\gamma_2)\left(1+\frac{Y}{2}\right)(1+Y)\right]\right\}, Y \equiv x\coth x,$$

$$\psi_0 = 3N\theta\left[x + \ln(1-e^{-2x})\right], x = \frac{\hbar\omega}{2\theta}, \omega = \sqrt{\frac{k}{m}}, \qquad (1)$$

where $U_0 = \frac{N}{2}u_0$ u_0 is the cohesive energy of an atom, N is the number of atoms in the metal, $\theta = k_B T$, k_B is the Boltzmann constant, T is the absolute temperature, $\hbar = \frac{h}{2\pi}$, h is the Planck constant, ω is the vibration frequency of

atom at lattice point node, k is the harmonic parameter of the metal, m is the atom mass, γ_1, γ_2 are anharmonic parameters of the metal [68].

The equations of state for f.c.c. metals at pressure P and temperature T and at P and $T = 0$ K respectively are determined by [69]

$$Pv = -r_1\left(\frac{1}{6}\frac{\partial u_0}{\partial r_1} + \theta Y\frac{1}{2k}\frac{\partial k}{\partial r_1}\right), \tag{2}$$

$$Pv = -a\left(\frac{1}{6}\frac{\partial u_0}{\partial a} + \frac{\hbar\omega}{2k}\frac{\partial k}{\partial a}\right), \tag{3}$$

where r_1 is the nearest neighbour distance and $v = \frac{V}{N} = \frac{\sqrt{2}r_1^3}{2}$ is the volume of cubic unit cell per atom for f.c.c. lattice. If knowing the form of interaction potential between two atoms, from Eq. (3) we can find the nearest neighbour distance $r_{01}(P,0)$ and the metal parameters $k(P,0)$, $\gamma_1(P,0)$, $\gamma_2(P,0)$, $\gamma(P,0)$, at temperature $T = 0$ K and pressure P. From that, we can determine the displacement $y(P,T)$ of an atom from the equilibrium position at temperature T and pressure P [68].

The nearest neighbour distance between two atoms $r_1(P,T)$ at temperature T and pressure P is given by [68]

$$r_1(P,T) = r_{01}(P,0) + y(P,T). \tag{4}$$

Absolute stability limit temperature for the crystalline state of the metal has the form [68–73]

$$T_S = \frac{r_{1S}}{18k_B\gamma_G(P,T_S)}\left(\frac{\partial u_0}{\partial r_1}\right)_{T=T_S} + \left(\frac{\partial T}{\partial P}\right)_v P, \tag{5}$$

where $r_{1S} = r_1(P,T_S)$ and $\gamma_G = -\frac{r_1}{6k}\frac{\partial k}{\partial r_1}Y$ is the Grüneisen parameter of the metal.

The melting temperature T_m of perfect metal is derived from the temperature T_S by the following expression [68–73]

$$T_m \approx T_S + \frac{r_{1m} - r_{1S}}{k_B\gamma_G(P,T_S)}\left\{\frac{Pv(P,T_S)}{r_{1S}} + \frac{1}{18}\left[\left(\frac{\partial u_0}{\partial r_1}\right)_{T=T_S} + r_{1S}\left(\frac{\partial^2 u_0}{\partial r_1^2}\right)_{T=T_S}\right]\right\}, \tag{6}$$

where $r_{1m} = r_1(P,T_m)$, $a_m = a(P,T_m)$. Eq. (6) is used to determine the meting temperature of perfect metal at $P = 0$.

The dependence of the melting temperature T_m on pressure P can be considered by a dislocation-mediated theory [74], which is written as

$$T_m(P) = T_m(0)\frac{G(P)}{G(0)}\left[\frac{B_T(P)}{B_T(0)}\right]^{-1/b}, \tag{7}$$

where G and B_T is the shearing modulus and *the* isothermal bulk modu-

lus, $b = \left(\frac{dB_T}{dP}\right)_{P=0}$. G and B_T are determined by the SMM as follows

$$G = \frac{k^5}{2\pi r_1(1+\nu)k^4 + \gamma^2\theta^2(Y+1)(Y+2)}, \tag{8}$$

$$B_T = -\frac{r_1(P,T)}{3}\left(\frac{\partial P}{\partial r_1}\right)_T \left[\frac{r_{01}(P,0)}{r_1(P,T)}\right]^3, \tag{9}$$

where ν is the Poisson ratio.

Thze equilibrium vacancy concentration of the metal is determined by the following expression [71, 73, 75]

$$n_\upsilon = \exp\left(\frac{u_0}{4\theta}\right). \tag{10}$$

Then, the melting temperature of defective metal can be written as [73, 76, 77]

$$T_m^R = T_m - \left(\frac{\partial T}{\partial n_\upsilon}\right)_{P,V} n_\upsilon(T_m) = T_m - \frac{T_m^2}{\frac{T_m}{4}\frac{\partial u_0}{\partial \theta} - \frac{u_0}{4k_{\text{Bo}}}}. \tag{11}$$

Eq. (11) only gives SMM predictions in the range of pressure from zero to 100 GPa [71, 73, 75].

Eq. (7) for the melting temperature of defective metals can be written as

$$T_m^R(P) = T_m^R(0)\frac{G^R(P)}{G^R(0)}\left[\frac{B_T^R(P)}{B_T^R(0)}\right]^{-1/b^R}, \tag{12}$$

where $b^R = \left(\frac{dB_T^R}{dP}\right)_{P=0}$ and

$$G^R = G - \frac{r_1 n_\upsilon}{2\nu(1+\nu)}\left[\frac{r_1}{4\theta}\left(\frac{\partial u_0}{\partial r_1}\right)^2\left(2+\frac{u_0}{4\theta}\right) + \left(r_1\frac{\partial^2 u_0}{\partial r_1^2} + \frac{1}{2}\frac{\partial u_0}{\partial r_1}\right)\left(1+\frac{u_0}{4\theta}\right)\right], \tag{13}$$

$$B_T^R = B_T + n_\upsilon n_1 \Delta B_T + n_\upsilon \frac{u_0}{4\psi_0} B_T, \tag{14}$$

where n_1, ΔB_T, ψ_0 are first coordination number in perfect lattice, vacancy-induced and the Helmholtz free energy per atom change in the isothermal bulk modulus [78].

The jump of volume at melting point for metal can be found from the following expression

$$\Delta\upsilon_m = \frac{\varepsilon\theta r_1^3}{\sqrt{2}k\langle u\rangle^2}\left(1 + \frac{6\gamma^2\theta^2}{k^4}\right), \tag{15}$$

where ε is a constant depending on the nature of metal and normally

takes the value 0.01 [76], $\langle u \rangle = y$ is the displacement of atom from the equilibrium position. In order to determine the jump of volume Δv_m at pressure P and temperature T, it is necessary to determine $r_1, \langle u \rangle$ at pressure P and temperature T. The metal parameters k, γ are determined with respect to r_1 at pressure P and temperature T.

After finding the melting curve $T_m(P)$, we can calculate the slope $\frac{\partial T_m}{\partial P}$ of this curve. Knowing T_m, $\frac{\partial T_m}{\partial P}$ and Δv_m, we can be derive the jump of enthalpy at melting point from the Clapeyron–Clausius equation

$$\Delta H_m = \frac{T_m \Delta v_m}{\frac{\partial T_m}{\partial P}} \tag{16}$$

and the jump of entropy at melting point

$$\Delta S_m = \frac{\Delta H_m}{T_m}. \tag{17}$$

The isothermal compressibility of the metal is determined by [68]

$$\chi_T(P,T) = \frac{3\left[\frac{r_1(P,T)}{r_{01}(P,0)}\right]^3}{2P + \frac{r_1^2(P,T)}{3V}\left(\frac{\partial^2 \psi}{\partial r_1^2}\right)_T},$$

$$\frac{1}{3N}\left(\frac{\partial^2 \psi}{\partial r_1^2}\right)_T = \frac{1}{6}\frac{\partial^2 u_0}{\partial r_1^2} + k_{\text{Bo}} T\left[\frac{Y}{2k}\frac{\partial^2 k}{\partial r_1^2} - \frac{1}{4k^2}\left(\frac{\partial k}{\partial r_1}\right)^2 (Y + Z^2)\right], Z \equiv \frac{x}{\sinh x} \tag{18}$$

The thermal expansion coefficient of the metal can be determined by the following expression [68]

$$\alpha_T(P,T) = -\frac{\sqrt{2}\chi_T(P,T)}{3r_1^2(P,T)}\frac{1}{3N}\frac{\partial^2 \psi}{\partial T \partial r_1},$$

$$\frac{1}{3Nk_{\text{Bo}}}\frac{\partial^2 \psi}{\partial T \partial r_1} = \frac{Z^2}{2k}\frac{\partial k}{\partial r_1} + \frac{2k_{\text{Bo}}T}{k^2}\left[\frac{\gamma_1}{3k}\frac{\partial k}{\partial r_1}(2 + YZ^2) - \right.$$

$$\left. - \frac{1}{6}\frac{\partial \gamma_1}{\partial r_1}(4 + Y + Z^2) - \left(\frac{2\gamma_2}{k}\frac{\partial k}{\partial r_1} - \frac{\partial \gamma_2}{\partial r_1}\right) YZ^2\right]. \tag{19}$$

The heat capacity at constant volume has the form [68]

$$C_V(P,T) = 3Nk_{\text{Bo}}\left\{Z^2 + \frac{2k_{\text{Bo}}T}{k^2}\left[\left(2\gamma_2 + \frac{\gamma_1}{3}\right)YZ^2 + \right.\right.$$

$$+\frac{\gamma_1}{3}(1+Z^2)-\gamma_2(Z^4+2Y^2Z^2)\Big]\Big\} \tag{20}$$

The Grüneisen parameter of the metal is calculated by [68]

$$\gamma_{\mathrm{G}}(P,T)=\frac{3\alpha_T(P,T)V(P,T)}{\chi_T(P,T)C_V V}. \tag{21}$$

The Debye temperature of the metal at pressure P is derived from [77]

$$T_{\mathrm{D}}(P)=T_{\mathrm{D0}}\exp\left\{-\frac{\gamma_{\mathrm{G0}}}{q}\left[\left(\frac{V}{V_0}\right)^q-1\right]\right\}, \tag{22}$$

where $T_{\mathrm{D0}}=\dfrac{4\hbar}{3k_{\mathrm{Bo}}}\sqrt{\dfrac{k(0,T)}{m}}$ is the Debye temperature of the metal at zero pressure, $V\equiv V(P,T)$, $V_0\equiv V0,T)$, $\gamma_G\equiv\gamma_G(P,T)$, $\gamma_{G0}\equiv\gamma_G(0,T)$, $q>0$ and q is a material constant.

The electrical resistivity of phonons is given by the Bloch–Grüneisen law [79]

$$\rho_E=\rho_0+\frac{B}{T_D}\left(\frac{T}{T_D}\right)^5\int_0^{T_D/T}\frac{z^5dz}{(e^z-1)(1-e^{-z})}, \tag{23}$$

where ρ_0,B and T_D respectively are the residual resistivity, the material constant and the Debye temperature. The constants ρ_0,B are determined from the experimental data. According to the Mott equation [80],

$$\rho_{EL}=\rho_{ES}\exp\left(\frac{80L_f}{T_m}\right), \tag{24}$$

where L_f is the latent heat of fusion; ρ_{EL} and ρ_{ES} are the electrical resistivities of liquid and solid phases. According to the Wiedemann–Franz law, the thermal conductivity of the metal is calculated by

$$\kappa=\frac{LT}{\rho_E}, \tag{25}$$

where $L=\dfrac{\pi^3}{3}\left(\dfrac{k_B}{e}\right)^2$ is the Lorentz number.

The thermal diffusivity λ is defined by

$$\lambda=\frac{\kappa}{\rho C_P}, \tag{26}$$

where ρ is the density and $C_P=C_V+\dfrac{9TV\alpha_T^2}{\chi_T}$ is the heat capacity at constant pressure.

2.2. Numerical Results and Discussions for Au

In order to study Au, we applied the Mie–Lennard-Jones (MLJ) pair interaction potential as follows [81, 82, 84]

$$\varphi(r) = \frac{D}{n-m}\left[m\left(\frac{r_0}{r}\right)^n - n\left(\frac{r_0}{r}\right)^m\right], \tag{27}$$

where parameters D and r_0 are determined from the experimental data and parameters m and n are by the empirical way. The MLJ potential parameters for the interaction Au–Au are given in Table 1.

The obtained numerical results of the melting temperature, the slope of the melting curve, the jumps of volume, enthalpy and entropy at the melting point, the thermal conductivity and the thermal diffusivity for

Table 1. **The MLJ potential parameters for Au**

Interaction	D/k_{Bo} (K)	r_0 (10^{-10} m)	m	n
Au–Au [81]	7411.5	2.8751	5.5	10.5

Table 2. **The melting temperature, the slope of the melting curve, the jumps of volume, enthalpy and entropy at the melting point for Au at $P = 0$ calculated by the SMM according to the perfect metal model in Figure 1**

T_m(K)	$\partial T_m/\partial P$ (K/ GPa)	Δv_m (E^3)	ΔH_m (meV)	ΔS_m (k_{Bo})
1341	57.77	4.78	163.6	0.1219

Table 3. **The temperature dependence of the jumps of volume, enthalpy and entropy for Au at $P = 0$**

T (K)	Δv_m (E^3)	ΔH_m (meV)	ΔS_m (k_{Bo})
100	8.78	297.32	0.222
200	4.56	154.47	0.116
300	3.16	106.95	0.079
500	2.07	70.03	0.052
700	1.66	56.14	0.042
800	1.56	52.78	0.039
900	1.5	50.92	0.038
1000	1.48	50.28	0.037
1100	1.5	50.67	0.037
1200	1.54	52.06	0.039

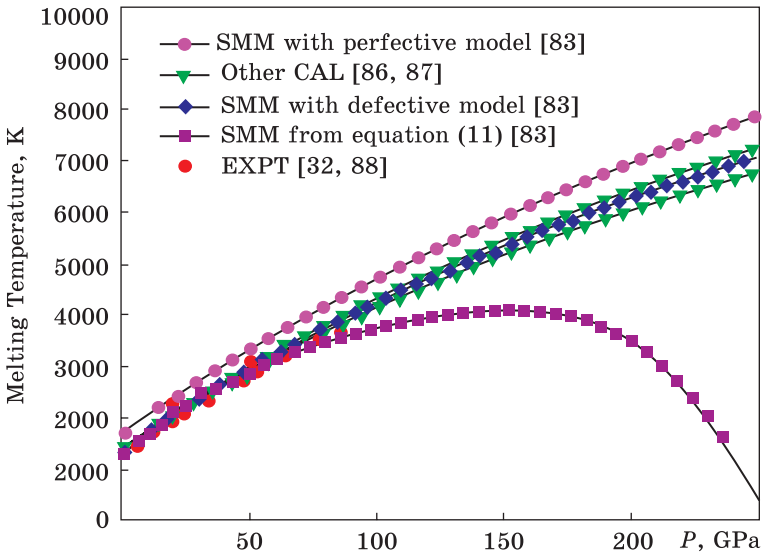

Fig. 1. The melting curve of Au calculated by the SMM according to the perfect metal model [83], the SMM according to the defective metal model [83], the SMM calculation from Eq. (11) [83], other calculations [86, 87] and experiments [32, 88]

Au in the temperature range of 0–1350 K and in the pressure range of 0–250 GPa are summarized in tables from Table 2 to Table 5 and are illustrated in figures from Figure 1 to Figure 6.

Figure 1 shows the correlations between pressure and the melting temperature of Au up to 250 GPa [83]. It is possible to reproduce accurately experimental results [32, 88] for Au in the range of pressure from zero to 100 GPa by using Eq. (11). However, this equation is invalidated when $P \geq 150$ GPa while the f.c.c.–b.c.c. phase transition

Table 4. **The temperature dependence of the heat capacity at constant pressure for Au at $P = 0$**

T(K)	100	300	500	700	800	1000	1200
C_p (cal/mol·K)	5.12	6.00	6.20	6.40	6.48	6.70	6.96
C_p (cal/mol·K) [89]	5.12	6.07	6.28	6.52	6.65	6.90	7.15

Table 5. **The pressure dependence of the thermal conductivity κ and the thermal diffusivity λ for Au at $T = 300$K**

P(GPa)	1	3	5	7	8	9
κ(10^{-6} W/mK)	117.67	313.81	330.38	332.22	332.47	332.59
λ(10^{-15} m^2/s)	57.670	42.182	24.068	16.119	13.721	11.897

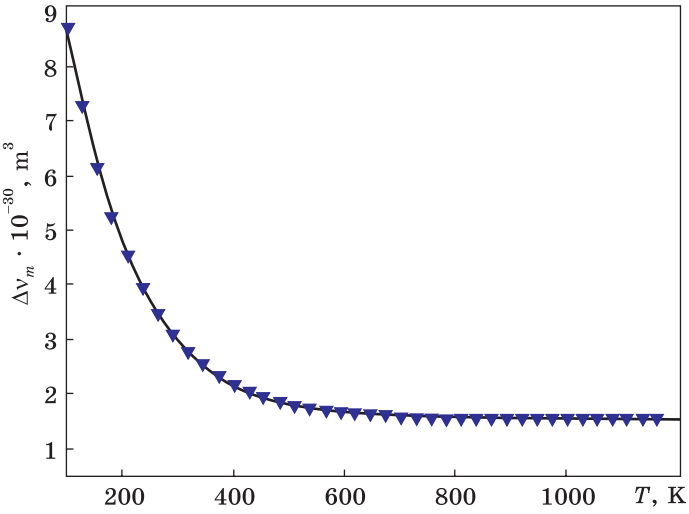

Fig. 2. $\Delta v_m(T)$ for Au at $P = 0$

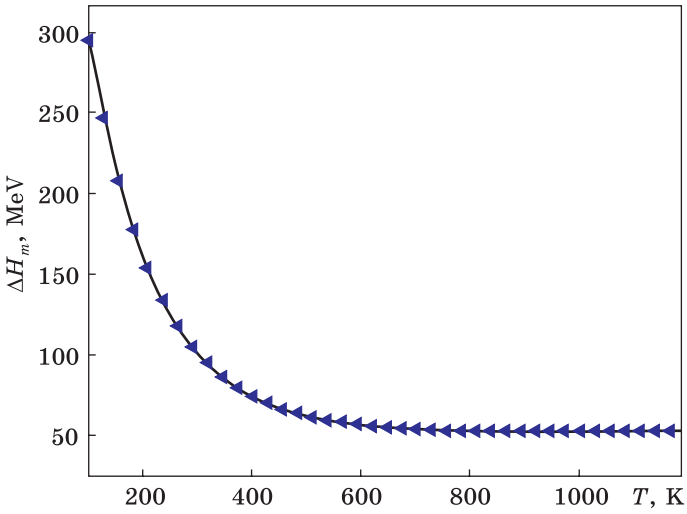

Fig. 3. $\Delta H_m(T)$ for Au at $P = 0$

pressure is reported to be approximately 240 GPa [85]. To understand a monotonous variation of the melting temperature with compression, we can employ the perfect model. Nevertheless, this if not an exact approximation. For example, the perfect model gives $T_m(0) = 1612$ K, which is 21% larger than the corresponding experimental value of 1335 K [32.88]. In contrast, combining Eqs. (11) and (12) provides relative error $\delta = \dfrac{T_m - T_m^R}{T_m} = 9.74\%$. This reduction brings a good agreement between the SMM calculation and comparable data [32, 85, 88]. We use the melting curve of Au calculated by the SMM according to the perfect metal model on Figure 1 in order to find the melting temperature

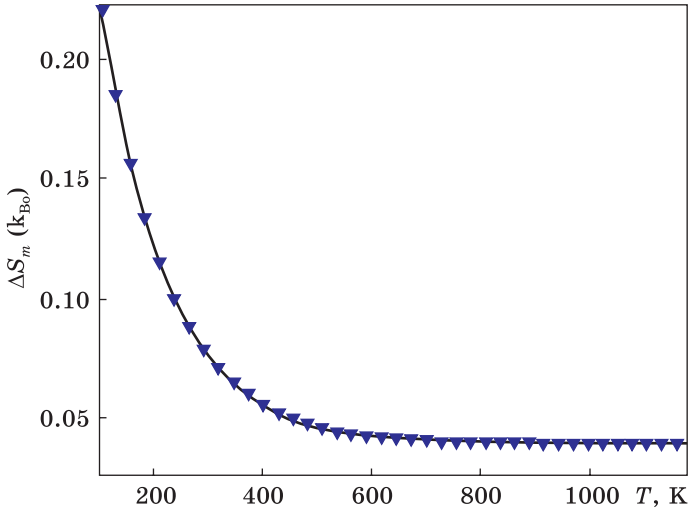

Fig. 4. $\Delta S_m(T)$ for Au at $P = 0$

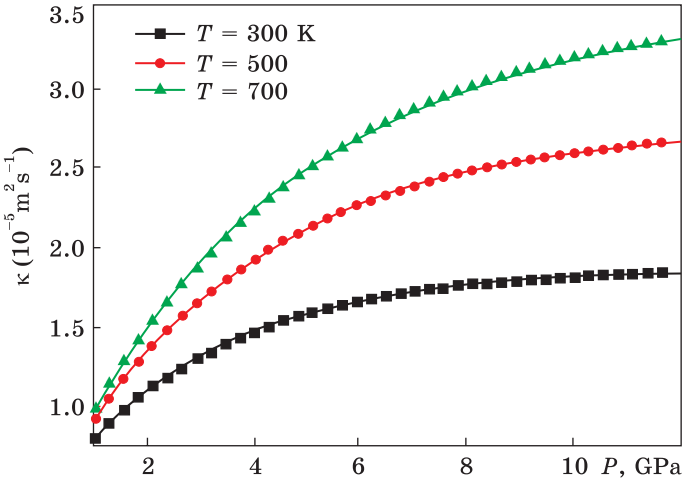

Fig. 5. $\kappa(T,P)$ for Au

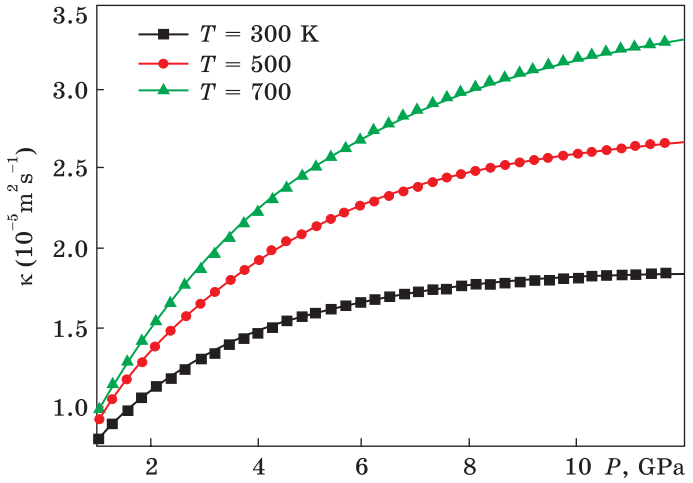

Fig. 6. $\lambda(T,P)$ for Au

T_m = 1341 K and the slope $\frac{\partial T_m}{\partial P} = 57.77$ K/GPa of the melting curve of Au at P = 0. By using Eq. (15), we can find the jump of volume Δv_m = 4.78 Å^3 at the melting point 1341 K. From the obtained values of $T_m, \frac{\partial T_m}{\partial P}, \Delta v_m$ and Eq. (16), we derive the jump of enthalpy ΔH_m = = 163.6 meV. From the obtained values of T_m, ΔH_m and Eq. (17), we determine the jump of entropy $\Delta S_m = 0.1219\, k_{\text{Bo}}$. These results are summarized in Table 2.

The temperature dependences (the melting temperature dependences) of the jumps of volume, enthalpy and entropy for Au at P = 0 and in the range of temperature from 100 to 1200 K are summarized in Table 3 and illustrated on figures from Figure 2 to Figure 4. Graphs $\Delta v_m(T)$, $\Delta H_m(T)$ and $\Delta S_m(T)$ have analogical forms. When temperature increases from 100 to 300 K, $\Delta v_m, \Delta H_m$ and ΔS_m strongly decrease. Still when temperature increases from 300 to 1200 K, $\Delta v_m, \Delta H_m$ and ΔS_m gradually decrease and then insignificantly change.

The temperature dependence of the heat capacity at constant pressure $C_P = C_V + \frac{9TV\alpha_T^2}{\chi_T}$ for Au at P = 0 calculated by the SMM is in good agreement with experiments as shown in Table 4.

Table 5 is the pressure dependence of the thermal conductivity κ and the thermal diffusivity λ for Au at T = 300 K and in the range of pressure from zero to 9 GPa. When pressure increases from 1 to 9 GPa, the thermal conductivity increases from $11.67 \cdot 10^{-6}$ to $332.59 \cdot 10^{-6}$ W/mK and the thermal diffusivity deceases from $57.67 \cdot 10^{-15}$ to $11.897 \cdot 10^{-15}$ m^2/s. The temperature and pressure dependences of the thermal conductivity κ and the thermal diffusivity λ for Au at temperatures T = 300, 500 and 700 K and in the range of pressure from 0 to 12 GPa are illustrated on Figure 5 and Figure 6. According to these figures, for Au at the same pressure when temperature increases, the thermal conductivity κ and the thermal diffusivity λ increase too. For Au at the same temperature when pressure increases, the thermal conductivity κ increases and the thermal diffusivity λ decreases.

In this paper, we applied the following formula for the electrical resistivity of Au [77]

$$\rho_E = 0.022 + \frac{1150}{T_D}\left(\frac{T}{T_D}\right)^5 \int_0^{T_D/T} \frac{z^5 dz}{(e^z - 1)(1 - e^{-z})}. \qquad (22)$$

These SMM calculated results of Hoc *et al*. [77] are completely consistent with the experimental results of Berrada [88] and Matula [80] at P = 0, T = 0—1350 K. In the range of high temperature ($T >> T_D$),

the electrical resistivity increases linearly in respect to temperature. In the range of low temperature ($T << T_D$), the electrical resistivity is proportional to T^6. This can be seen through Eq. (22). In the range of temperature from zero to 1350 K and in the range of pressure from 0 to 5 GPa, the SMM calculations are in good agreement with other theoretical calculations and the experimental data. The SMM calculations of electrical resistivity for Au at high pressures up to 100 GPa in [77] orient and predict experimental data in the future. Because our SMM calculations of electrical resistivity for in [77] are reliable and the SMM calculations of the heat capacity at constant pressure for Au calculated by the SMM is in good agreement with experiments, our SMM calculations of thermal conductivity and thermal diffusivity also are reliable. Our SMM calculations of the jumps of volume, enthalpy and entropy, the thermal conductivity and the thermal diffusivity for Au can be extended for the range of temperature from zero to 1350 K and the range of pressure from zero to 100 GPa as in our previous paper [77].

3. Conclusion

The melting temperature, the jumps of volume, enthalpy and entropy at the melting point, the isothermal compressibility, the thermal expansion coefficient, the heat capacity at constant volume, the Grüneisen parameter, the Debye temperature, the electrical resistivity, the thermal conductivity and the thermal diffusivity for f.c.c. defective and perfect metals are studied by combining the statistical moment method (SMM), the limiting condition of the absolute stability of the crystalline state, the Clapeyron–Clausius equation, the Debye model, the Grüneisen equation, the Wiedemann–Franz law and the Mott equation. Our numerical calculations of obtained theoretical results are carried out for Au under high temperature up to 1200 K and pressure up to 12 GPa. The SMM calculated melting curve of Au is in good agreement with experiments and other calculations. Our calculations for the jumps of volume, enthalpy and entropy, the thermal conductivity and the thermal diffusivity for Au predict and orient experimental results in the future.

REFERENCES

1. D. Batani, A. Balducci, D. Beretta, A. Bernardinello, T. Lцwer, M. Koenig, A. Benuzzi, B. Faral, and T. Hall, Equation of state data for gold in the pressure range <10 TPa, *Phys. Rev. B*, **61**, No.14: 9287 (2000); 10.1103/PhysRevB.61.9287
2. K. Takemura and A. Dewaele, Isothermal equation of state for gold with a He-pressure medium, *Phys. Rev. B*, **78**: 104119 (2008); https://doi.org/10.1103/PhysRevB.78.104119
3. A. Dewaele, P. Loubeyre, F. Occelli, O. Marie, and M. Mezouar, Toroidal diamond anvil cell for detailed measurements under extreme static pressures, *Nat. Com*

mun., **9**: 2913 (2018);
https://doi.org/10.1038/s41467-018-05294-2
4. M.C. Daniel; D. Astruc, Gold Nanoparticles: Assembly, Supramolecular Chemistry, Quantum-Size-Related Properties, and Applications toward Biology, Catalysis, and Nanotechnology, *Chem. Rev*, **104**, No.1: 293-346 (2004);
https://doi.org/10.1021/cr030698+
5. P. Song; L.C. Cai; Q.S. Wang; X.M. Zhou; X.Z. Li; Y. Zhang; S. Yuan; J.D. Weng, and J. B. Li, Sound velocity, temperature, melting along the Hugoniot and equation of state for two porosity aluminums, *J. Appl. Phys*, **110**: 103522 (2011); https://doi.org/10.1063/1.3662193
6. A. Dewaele; M. Mezouar; N. Guignot, and P. Loubeyre, High Melting Points of Tantalum in a Laser-Heated Diamond Anvil Cell, Phys. *Rev. Lett*, **104**: 255701 (2010);
https://doi.org/10.1103/PhysRevLett.104.255701
7. J.H. Zhu; Q.S. Fu; Y.Q. Xue; Z.X. Cui, Comparison of different models of melting transformation of nanoparticles, *J. Mater. Sci*., **51**: 4462. (2016);
https://doi.org/10.1007/s10853-016-9758-1
8. C.C. Yang; Y.-W. Mai, Thermodynamics at the nanoscale: A new approach to the investigation of unique physicochemical properties of nanomaterials, *Mater. Sci. Eng.*, R, **79**: (2014);
https://doi.org/10.1016/j.mser.2014.02.001
9. Z.H. Li; D.G. Truhlar, Nanothermodynamics of metal nanoparticles, *Chem. Sci.*, **5**: 2605 (2014);
https://doi.org/10.1039/C4SC00052H
10. G. Kaptay, J. Janczak-Rusch, G. Pigozzi, L.P.H. Jeurgens, Theoretical Analysis of Melting Point Depression of Pure Metals in Different Initial Configurations, *J. Mater. Eng. Perform*. 2014, **23**, No.5: 1600-1607 (2014);
https://doi.org/10.1007/s11665-014-0885-z
11. F. Font; T.G. Myers; S.L. Mitchell, A mathematical model for nanoparticle melting with density change, *Microfluid. Nanofluid*, **18**: 233 (2015);
https://doi.org/10.1007/s10404-014-1423-x
12. D. Alfи, Temperature of the inner-core boundary of the Earth: Melting of iron at high pressure from first-principles coexistence simulations, *Phys. Rev. B*, **79**: 060101(R). (2009);
https://doi.org/10.1103/PhysRevB.79.060101
13. J. Bouchet; F. Bottin; G. Jomard, and G. Zйrah, Melting curve of aluminum up to 300 GPa obtained through *ab initio* molecular dynamics simulations, *Phys. Rev.B*, **80**: 094102 (2009);
https://doi.org/10.1103/PhysRevB.80.094102
14. V. Stutzmann; A. Dewaele; J. Bouchet; F. Bottin, and M. Mezouar, High-pressure melting curve of titanium, *Phys. Rev. B*, **92**: 224110 (2015);
https://doi.org/10.1103/PhysRevB.92.224110
15. J.Q. Broughton and X.P. Li, Phase diagram of silicon by molecular dynamics, *Phys. Rev. B*, **35**: 9120 (1987);
https://doi.org/10.1103/PhysRevB.35.9120
16. A.B. Belonoshko; N.V. Skorodumova; A. Rosengren, and B. Johansson, Melting and critical superheating, *Phys. Rev. B*, **73**: 012201 (2006);
https://doi.org/10.1103/PhysRevB.73.012201
17. F.A. Lindemann, The calculation of molecular vibration frequency, *Physik. Z*, **11**: 609 (1910)
18. H.K. Hieu and N.N. Ha, High pressure melting curves of silver, gold and copper, *AIP Adv*, **3**: 112125 (2013);
https://doi.org/10.1063/1.4834437

19. N.A. Smirnov; Y.M. Chen; X.R. Chen, and Q. Wu, *J. Phys.: Condens. Matter*, **29**: 105402 (2017);
https://doi.org/10.1088/1361-648X/aa58ca
20. Q. An; S.N. Luo; L.B. Han; L. Zheng and O. Tschauner, Melting of Cu under hydrostatic and shock wave loading to high pressures, *Journal of Physics: Condensed Matter*, **20**, No.9: 095220 (2008);
https://doi.org/10.1088/0953-8984/20/9/095220
21. J.B. Adams; S.M. Foiles, and W.G. Wolfer, Self-diffusion and impurity diffusion of fee metals using the five-frequency model and the Embedded Atom Method, *J. Mater. Res*, **4**: 102. (1989);
https://doi.org/10.1557/JMR.1989.0102
22. P. Pawlow, The dependency of the melting point on the surface energy of a solid, *Z. Phys. Chem., Stoechiom. Verwandtschaftsl*, **65**: 545 (1909);
23. E. Rie, Influence of surface tension on melting and freezing, *Z. Phys. Chem., Stoechiom. Verwandtschaftsl*, **104**: 354 (1923).
24. D. Errandonea; B. Schwager; R. Ditz, C. Gessmann; R. Boehler and M. Ross, Systematics of transition-metal melting. *Physical Review B*, **63**, No.13: 132104, (2001);
https://doi.org/10.1103/PhysRevB.63.132104
25. S.N. Luo and T.J. Ahrens, Shock-induced superheating and melting curves of geophysically important minerals, *Physics of the Earth and Planetary Interiors*, **143**: 369-386 (2004);
https://doi.org/10.1016/j.pepi.2003.04.001
26. P. Buffat; J.-P. Borel, Size effect on the melting temperature of gold particles, *Phys. Rev. A*, **13**: 2287 (1976);
https://doi.org/10.1103/PhysRevA.13.2287
27. S. Pratontep, S.J. Carroll, C. Xirouchaki, M. Streun, R.E. Palmer, *Rev. Sci. Instrum*. **76**, No. 9: (2005);
https://doi.org/10.1063/1.1869332
28. B.K. Godwan; A. Ng and L. Dasilva, Melting and Hugoniot calculations for gold, *Physical Letters A*, **144**: 26-30 (1990);
https://doi.org/10.1016/0375-9601(90)90042-M
29. A. Migault; J. P. Jamain and J. Jacquesson, Fusion curves at high pressure and arameter Grüneisen of metals, In *Proc. 7 Int.AIRAPT conf. high presure science technology*, Oxford, **2**: 938-944 (1980)
30. V.V. Hung and N.T. Hai, Investigation of the melting temperature of metal at various pressures, *Journal of the Physical Society of Japan*, **66**: 3499-3501 (1997);
https://doi.org/10.1143/JPSJ.66.3499
31. J. Akella and G.C. Kennedy, Melting of Au, Ag and Cu-proposal for a new hogh-pressure calibration scale, *Journal of Geophysical Research*, **76**: 4969-4977 (1971);
https://doi.org/10.1029/JB076i020p04969
32. P.W. Mirwald and G.C. Kennedy, The melting curve of Au, Ag and Cu to 60 −kbar pressure. A reinvestigation, *Journal of Geophysical Research*, **84**: 6750-6756 (1979)
https://doi.org/10.1029/JB084iB12p06750
33. T. Sumita; M. Kato and A. Yoneda, The thermal analysis in an MA-8 type apparatus: the melting of gold at 12 GPa, *The review of high pressure science and technology*, ed. by M.Nakahara, **7**: 254-256 (1998);
34. B. Roldan Cuenya, M. Alcántara Ortigoza, L.K. Ono, F. Behafarid, S. Mostafa, J.R. Croy, K. Paredis, G. Shafai, T.S. Rahman, L.Li, Z. Zhang, J.C. Yang, Thermodynamic properties of Pt nanoparticles: Size, shape, support, and adsorbate

effects, *Phys. Rev. B*, **84**: 245438 (2011);
https://doi.org/10.1103/PhysRevB.84.245438
35. O.A. Yeshchenko, I.M. Dmitruk, A.A. Alexeenko, A.M. Dmytruk, Size-dependent melting of spherical copper nanoparticles embedded in a silica matrix, *Phys. Rev. B*, **75**: 085434 (2007);
https://doi.org/10.1103/PhysRevB.75.085434
36. Wenjuan Zhang; Yongqiang Xue; Qingshan FuZixiang; CuiShuting Wang, Size dependence of phase transition thermodynamics of nanoparticles: A theoretical and experimental study, *Powder Technology*, **308**, 258-265 (2017);
https://doi.org/10.1016/j.powtec.2016.11.052
37. Q.S. Fu; Z.X. Cui; Y.Q. Xue; H.J. Duan, Research of Size- and Shape-Dependent Thermodynamic Properties of the Actual Melting Process of Nanoparticles, *J. Phys. Chem. C*, **122**, No 27: 15713 (2018);
https://doi.org/10.1021/acs.jpcc.8b03085
38. Z.X. Cui; M.Z. Zhao; W.P. Lai; Y.Q. Xue, Thermodynamics of Size Effect on Phase Transition Temperatures of Dispersed Phases, *J. Phys. Chem. C*, **115**, No. 45, 22796 (2011);
https://doi.org/10.1021/jp2067364
39. D. Errandonea, Phase behavior of metals at very high P– T conditions: A review of recent experimental studies, *J. Phys. Chem. Solids*, **67**, 2017 (2006);
https://doi.org/10.1016/j.jpcs.2006.05.031
40. D. Errandonea; S.G. MacLeod; J. Ruiz-Fuertes; L. Burakovsky; M.I. McMahon; C.W. Wilson; J. Ibacez; D. Daisenberger; C. Popescu, High-pressure/high-temperature phase diagram of zinc, *Journal of Physics: Condensed*, 30: 295402 (2018);
https://orcid.org/0000-0003-0189-4221
41. P.I. Dorogokupets, Thermodynamics and equations of state of Iron to 350 GPa ad 6000 K, *Scientific Reports*, **7**: 41863 (2017);
https://doi.org/10.1038/srep41863
42. H.K. Hieu; N.N. Ha, High pressure melting curves of silver, gold and copper, *AIP Advances*, **3**: 112125 (2013); https://doi.org/10.1063/1.4834437
43. D. McLachlan Jr.; E.G. Ehlers, Effect of pressure on the melting temperature of metals, *J. Geophysical Research*, **76**, 2780 (1971);
https://doi.org/10.1029/JB076i011p02780
44. J. Shanker; M. Kumar; Thermodynamic Approximations in High-pressure and High-Temperature Physics of Solids, *Physica Status Solidi B*, **179**: 351 (1993);
https://doi.org/10.1002/pssb.2221790209
45. K. Kholiya; J. Chandra, A theoretical model to study melting of metals under pressure, *Modern Physics Letters B*, **29**: 1550161(1-13), (2015);
https://doi.org/10.1142/S0217984915501614
46. O.L. Anderson, *Equation of state for Geophysics and Ceramic Science*, Oxford University Press, Oxford, (1995);.
47. L. Dubrovinsky; N. Dubrovinskaia; W. A. Crichton; A. S. Mikhaylushkin; S. I. Simak; I. A. Abrikosov; J. S. de Almeida; R. Ahuja; W. Luo, and B. Johansson, Noblest of All Metals Is Structurally Unstable at High Pressure, *Phys.Rev.Lett*, **98**: 045503 (2007);
https://doi.org/10.1103/PhysRevLett.98.045503
48. S. T. Weir; D. D. Jackson; S. Falabella; G. Samudrala, and Y. K. Vohra, An electrical microheater technique for high-pressure and high-temperature diamond anvil cell experiments, *Rev. Sci. Instrum*, **80**: 013905 (2009);
https://doi.org/10.1063/1.3069286

49. C.S. Zha and W. A. Bassett, Internal resistive heating in diamond anvil cell for *in situ* x-ray diffraction and Raman scattering, *Rev. Sci. Instrum*, **74**: 1255 (2003)
https://doi.org/10.1063/1.1539895
50. T. Pippinger; L. Dubrovinsky; K. Glazyrin, R. Miletich, and N. Dubrovinskaia, *Fнsica de la Tierra*, **23**, 29 (2011); arXiv:1104.1304v1
51. Nguyen Trong Dung, Influence of impurity concentration, atomic number, temperature and tempering time on microstructure and phase transformation of Ni***1-x***Fe***x*** (**x** = 0:1, 0.3, 0.5) nanoparticles, Modern Physics Letters B, 32, No. 18, 1850204, 1850204 (2018);
https://doi.org/10.1142/S0217984918502044
52. Tran Quoc Tuan; Nguyen Trong Dung,_Effect of heating rate, impurity concentration of Cu, atomic number, temperatures, time annealing temperature on the structure, crystallization temperature and crystallization process of Ni***1-x***Cu***x*** bulk; **x** = 0.1, 0.3, 0.5, 0.7", International Journal of Modern Physics B, 32, No. 26: 1830009 (2018);
https://doi.org/10.1142/S0217979218300098
53. Dung Nguyen Trong, Kien Pham Huu, Phuong Nguyen Tri, Simulation on the factors affecting the crystallization process of FeNi alloy by Molecular Dynamics, *ACS Omega*, **4**: 14605-14612 (2019);
https://doi.org/10.1021/acsomega.9b02050
54. Nguyen Quang Hoc; Le Hong Viet; Nguyen Trong Dung, On the Melting of Defective FCC Interstitial Alloy c −FeC under Pressure up to 100 GPa, *Journal of Electronic Materials*, **49**, 910–916 (2020).
https://doi.org/10.1007/s11664-019-07829-9
55. Nguyen Trong Dung, Nguyen Chinh Cuong, Duong Quoc Van, Study on the effect of doping on lattice constant and electronic structure of bulk AuCu by the density functional theory, *Journal of Multiscale Modelling*, **11**, No. 2, 2030001 (2020)
https://doi.org/10.1142/S1756973720300014
56. Nguyen Trong Dung, Nguyen-Tri Phuong, Factors affecting the structure, phase transition and crystallization process of AlNi nanoparticles, *Journal of Alloys and Compounds*, **812**: 152133 (2020)
https://doi.org/10.1016/j.jallcom.2019.152133
57. Dung Nguyen Trong; Phuong Nguyen-Tri, Molecular dynamic study on factors influencing the structure, phase transition and crystallization process of NiCu6912 nanoparticle, *Materials Chemistry and Physics*, **250**: 123075 (2020);
https://doi.org/10.1016/j.matchemphys.2020.123075
58. Van Cao Long; Van Duong Quoc; and Dung Nguyen Trong, Ab Initio Calculations on the Structural and Electronic Properties of AgAu Alloys, *ACS Omega*, **5**, No. 48: 31391–31397 (2020); 10.1021/acsomega.0c04941
59. Dung Nguyen Trong; Van Cao Long and Ștefan Tălu, The Structure and Crystallizing Process of NiAu Alloy: A Molecular Dynamics Simulation Method, *J. Compos. Sci*, **5**, No. 1, 18 (2021);
https://doi.org/10.3390/jcs5010018
60. Dung NguyenTrong, Z-AXIS deformation method to investigate the influence of system size, structure phase transition on mechanical properties of bulk nickel, *Materials Chemistry and Physics*, **252**: 123275 (2020);
https://doi.org/10.1016/j.matchemphys.2020.123275
61. Tuan Tran Quoc; Dung Nguyen Trong, and Ștefan Tălu, Study on the Influence of Factors on the Structure and Mechanical Properties of Amorphous Alumin-

ium by Molecular Dynamics Method, *Advances in Materials Science and Engineering*, **2021**, 5564644 (2021);
https://doi.org/10.1155/2021/5564644
62. L. Vočadlo and D. Alfи, Ab initio melting curve of the fcc phase of aluminum. *Physical Review B*, **65** No. 21: 214105 (2002);
https://doi.org/10.1103/PhysRevB.65.214105
63. C.M. Liu; X.R. Chen; C. Xu, L.C. Cai and F.Q. Jing, Melting curves and entropy of fusion of body-centered cubic tungsten under pressure, *Journal of Applied Physics*, **112**: 013518 (2012);
https://doi.org/10.1063/1.4733947
64. S. Kumar; K.S. Nisar; R. Kumar; C. Cattani; B. Samet, A new Rabotnov fractional-exponential function based fractional derivative for diffusion equation under external force, *Mathematical Methods in Applied Science*, **43**: (2020);
https://doi.org/10.1002/mma.6208
65. M. Jleli; S. Kumar; R. Kumar; B. Samet; Analytical approach for time fractional wave equations in the sense of Yang-Abdel-Aty-Cattani via the homotopy perturbation transform method, *Alexandria Engineering Journal*, **59**, No. 5: (2020);
https://doi.org/10.1016/j.aej.2019.12.022
66. S. Kumar; A. Kumar; S. Abbas; M.A. Qurashi, A modifi ed analytical approach with existence and uniqueness for fractional Cauchy reaction-diffusion equations, *Advances in Difference Equations*, **2020**, 28 (2020).
https://doi.org/10.1186/s13662-019-2488-3
67. S. Kumar; R. Kumar; R.P. Agarwal; B. Samet, A study on fractional Lotka-Volterra population model by using Haar wavelet and Adam's-Bashforth-Moulton methods, *Mathematical Methods in Applied Science*, **43**, No. 8: (2020);
https://doi.org/10.1002/mma.6297
68. N. Tang and V.V. Hung, Investigation of the thermodynamic properties of anharmonic crystals by the momentum method, (I) General results for FCC crystals, *Phys. Stat. Sol. (b)*, **149**: 511-519 (1988);
https://doi.org/10.1002/pssb.2221490212
69. L.T.C. Tuyen; N.Q. Hoc; B.D. Tinh; D.Q. Vinh and T.D. Cuong, Study on the melting of interstitial alloys FeH and FeC with BCC structure under pressure, *Chinese Journal of Physics,* **59**: (2019);
https://doi.org/10.1016/j.cjph.2019.02.018
70. T.D. Cuong; N.Q. Hoc and P.D. Anh, Application of the Statistical Moment Method to Melting Properties of Ternary Alloys with FCC Structure, *Journal of Applied Physics,* **125**, 215112 (2019);
https://doi.org/10.1063/1.5089228
71. V.V. Hung; D.T. Hai and L.T.T. Binh, Melting curve of metals with defect: Pressure dependence, *Computational Materials Science,* **79**, 789–794 (2013) 10.1016/j.commatsci.2013.07.042
72. N.Q. Hoc; L.H. Viet and N.T. Dung, On the melting of defective FCC interstitial alloy FeC under pressure up to 100 GPa, *Journal of Electronic Materials,* **49**: 910–916 (2020);
https://doi.org/10.1007/s11664-019-07829-9
73. N.Q. Hoc; T.D. Cuong; B.D. Tinh and L.H. Viet, Study on the melting of defective interstitial alloys TaSi and WSi with BCC structure, *Journal of Korean Physical Society,* **2019**, 71(8), 801-805.
74. L. Burakovsky; D.L. Preston and R.R. Silbar, Analysis of dislocation mechanism for melting of elements: Presure dependence, *Journal of Applied Physics*, **88**, 6294-6301 (2000) 10.1063/1.1323535

75. N.Q. Hoc; T.D. Cuong; B.D. Tinh and L.H. Viet, High-pressure melting curves of FCC metals Ni, Pd and Pt with defects, *Modern Physical Letters B*, **33**, No. 25: 1950300(2019);
https://doi.org/10.1142/S0217984919503007 .
76. V.V. Hung, Investigation of the change in volume, entropy and specific heat for metals on melting. *Proc. the 22nd National Conference of Theoretical Physics, Do Son, 3-5 August*, **1997**, 199-203.
77. N.Q. Hoc; B.D. Tinh and N.D. Hien, Influence of temperature and pressure on the electrical resistivity of gold and copper up to 1350K and 100GPa, *Materials Research Bulletin*, **128**, 110874 (2020);
https://doi.org/10.1016/j.materresbull.2020.110874
78. V.V. Hung; L.D. Thanh and N.T. Huong, Study of Elastic Moduli of Semiconductors with Defects by the Statistical Moment Method, *e-Journal of Surface Science and Nanotechnology*, 9, 499-502 (2011);
https://doi.org/10.1380/ejssnt.2011.499
79. H.K. Hieu; T.T. Hai; N.T. Hong; N.D. Sang and N.V. Tuyen, Electrical resistivity and thermodynamic properties of iron under high pressure, *Journal of Electronic Materials*, **46**, 3702–3706 (2017).
https://doi.org/10.1007/s11664-017-5411-2
80. R.A. Matula, Electrical resistivity of copper, gold, palladium, and silver, *Journal of Physical and Chemical Reference Data*, **8**, 1147 (1979);
https://doi.org/10.1063/1.555614
81. M.N. Magomedov, On calculating the Debye temperature and the Grüneisen parameter, *Zhurnal Fizicheskoi Khimii*, **1987**, 61(4), 1003-1009 (in Russian)
82. M.N. Magomedov, The calculation of the parameters of the Mie-Lennard-Jones potential, *High Temperature,* **44**, 513–529 (2006);
https://doi.org/10.1007/s10740-006-0064-583
83. T. D. Cuong; P.D. Anh, Modification of the statistical moment method for the high-pressure melting curve by the inclusion of thermal vacancies, *Vacuum*, **179**, 109444 (2020), arXiv:2005.06697
84. H.K. Hieu; N.N. Ha, High pressure melting curves of silver, gold and coppedr, *AIP Advances*, **2017**, 3, 112125.
85. N.A. Smirnov, *Journal of Physics: Condensed Matter*, **2013**, 76, 105402().
86. G. Weck; V. Recoules; J.A. Queyroux; F. Datchi; J. Bouchet; S. Ninet; G. Garbarino; M. Mezouar and P. Loubeyre, Determination of the melting curve of gold up to 110 GPa, *Physical Review B*, **101**, 014106(2020);
https://doi.org/10.1103/PhysRevB.101.014106
87. D. Errandonea, The melting curve of ten metals up to 12 GPa and 1600K, *Journal of Applied Physics*, **2010**, 108, 033517.
88. M. Berrada; R.A. Secco and W. Yong, Decreasing electrical resistivity of gold along the melting boundary up to 5 GPa, *High Pressure Research: An International Journal*, **108**, 033517 (2010);
https://doi.org/10.1063/1.3468149
89. McGraw-Hill, *American Institute of Physics Hand Book*, New York, 1963

Received 22.07.2021;
in final version, 01.11.2021

Н.К. Хок, Б.Д. Тін, Н.Д. Хієн, Л.Х. В'єт
[1] Національний університет освіти Ханоя, Ханой, В'єтнам
[2] Вища школа Мак Дінь Чі, провінція Залай, В'єтнам
[3] Університет Чан Куок Туан, Ханой, В'єтнам

ПРО СТРИБКИ ОБ'ЄМУ, ЕНТАЛЬПІЇ Й ЕНТРОПІЇ ЗА ТЕМПЕРАТУРИ ТОПЛЕННЯ, ТЕПЛОПРОВІДНІСТЬ І ТЕРМОДИФУЗІЮ ДЛЯ ГЦК-Au: ЗАЛЕЖНОСТІ ВІД ТЕМПЕРАТУРИ ТА ТИСКУ

Досліджуються температура топлення, стрибки об'єму, ентальпії та ентропії в точці топлення, ізотермічна стисливість, коефіцієнт теплового розширення, теплоємність при постійному об'ємі, Ґрюнайзенів параметер, Дебайова температура, питомий електричний опір, теплопровідність і термодифузія для ГЦК-металів з дефектами та ідеальних шляхом поєднання методи статистичних моментів, граничної умови абсолютної стабільности кристалічного стану, рівняння Клапейрона–Клаузіуса, Дебайового моделю, Ґрюнайзенового рівняння, закону Відемана–Франца, Моттового рівняння. Проведено чисельні розрахунки для Au за високих температур і тисків. Розрахована крива топлення Au добре узгоджується з експериментами й іншими розрахунками. Одержані результати є прогнозними та спонукають до нових експериментів.

Ключові слова: стрибки об'єму, ентальпія й ентропія за температури топлення, теплопровідність, теплопровідність, метод статистичних моментів.